Short Range United Atom Potentials for Alkanes: Decane and Nonane

S. Supple[a]; N. Quirke[a]

[a] Department of Chemistry, Imperial College of Science, Technology and Medicine, South Kensington, UK

PLEASE SCROLL DOWN FOR ARTICLE

Short Range United Atom Potentials for Alkanes: Decane and Nonane

S. SUPPLE and N. QUIRKE*

Department of Chemistry, Imperial College of Science, Technology and Medicine, South Kensington SW7 2AY, UK

The usefulness of a computational model can be judged not only by how accurately it reproduces experimental data but also how rapidly. Building on previous work by Smit *et al.* ["Computer simulations of vapor–liquid phase equilibria of *n*-alkanes," *J. Chem. Phys.*, 102 (1995) 2126], we investigate a short range potential for decane and nonane, with cut off distances R_c down to 6 Å. We found that at $R_c = 8$ Å (or $2.04\sigma_{CH_2}$) united atom potentials can be determined which are capable of providing an accurate description not only of alkane bulk phase behaviour but also interfacial properties.

INTRODUCTION

Despite their chemical simplicity the alkanes pose a number of challenges to physical chemists. For example, the problem of chain folding finds it simplest expression in the determination of the longest un-branched alkane with a linear global minimum, still an unsolved problem [1]. Alkane chains are of interest in modelling lipid molecules forming membranes [2–4]. In the limit of very long chains, polyethylene, is of tremendous theoretical and practical importance, not only from the point of view of understanding the origin and formation of its semi-crystalline structure [5] but also for the resulting physical properties including optical [6], mechanical [7,8] and electrical [9,10] behaviours. Clearly the phase behaviour of alkanes is also of interest (in particular to the oil industry), however, despite rapid progress [11–18] it is still not easy to quickly and reliably predict phase diagrams, especially for mixtures [19,20], from molecular models. One consideration is the computer time

required to calculate the pair interactions in the model fluid. For the study of adsorption [21] and wetting phenomena [22,23], where in addition, we have the interaction with the surface and where long equilibration times are required, the need to reduce computing time at each step becomes acute.

Many of these problems are modelled using a united atom description in which it is assumed that each CH_2 or CH_3 group can be described by a single interaction site or "united atom". These include models by Ryckaert and Bellemans [24] who created a model for liquid butane, Paul *et al.* [25] who performed calculations on polymethylene melts, Neubauer *et al.* [26] who studied the liquid–vapour phase behaviour of some cyclic-alkanes and Smit *et al.* [12] who compared a variety of models including one by Toxvaerd [27,28] which used an anisotropic united atom (AUA) potential designed to include the positional effect of the hydrogen atoms. Ungerer *et al.* later optimised this AUA potential [29].

Although these descriptions are accurate, many of them are relatively long range with cut-off lengths R_c of 13 Å or more. The greater the cut off the more interactions are taken into account and so the longer the calculation. What is required for many applications is a short-range potential that will reduce computational time while still giving accurate predictions.

In this paper, we look for the minimum value of the cut off R_c within the united atom model that is able to produce an accurate description of the phase behaviour and interfacial properties of two long chain alkanes—decane and nonane.

---

*Corresponding author. E-mail: n.quirke@ic.ac.uk

TABLE I   Values for the Lennard–Jones parameter ε for various cut off distances

	Decane				Nonane
Cut-off (R_c)	13.8 Å	11.0 Å	8.0 Å	6.0 Å	8.0 Å
ε_{CH2}	0.40725	0.43658	0.56930	1.26412	0.56930
ε_{CH3}	0.98780	1.05893	1.38085	3.06617	1.38085
$\varepsilon_{CH2/CH3}$	0.63426	0.67993	0.88663	1.96876	0.88663

All values are given in kJ mol^{-1}.

POTENTIALS

The model is based on that developed by Smit *et al.* [12] and is of the united atom type. The inter-molecular interactions consist of bond bending and torsion. The bond lengths are fixed at 1.53 Å. The bond bending is described by a harmonic Ploeg and Berendsen [30] potential

$$u^{\text{bend}}(\theta) = \frac{1}{2}k_\theta(\theta - \theta_0)^2 \qquad (1)$$

where $k_\theta = 519.66$ kJ mol^{-1} rad^{-2}, and the equilibrium angle, $\theta_0 = 114°$. For the torsion a triple cosine potential was used

$$u^{\text{tors}}(\phi) = \frac{1}{2}A_1(1 + \cos\phi) + \frac{1}{2}A_2(1 - \cos(2\phi))$$

$$+ \frac{1}{2}A_3(1 + \cos(3\phi)) \qquad (2)$$

where ϕ is the angle between the planes *ijk* and *jkn* (where *i*, *j*, *k* and *n* are consecutive adjacent atoms) and $A_1 = 2.9517$ kJ mol^{-1}, $A_2 = -0.56697$ kJ mol^{-1} and $A_3 = 6.5793$ kJ mol^{-1}. The forces F_{ij}, due to non-bonded interactions were modelled using the Lennard–Jones (12–6) potential, with $F_{ij} = -\partial u^{\text{LJ}}(r_{ij})/\partial r_{ij}, r < r_{\text{cut}}, = 0$ $r \geq r_{\text{cut}}$ corresponding to[†]

$$u^{\text{LJ}}(r_{ij}) = 4\varepsilon_{ij}[(\sigma_{ij}/r_{ij})^{12} - (\sigma_{ij}/r_{ij})^6] - u^{\text{LJ}}(r_{\text{cut}}) \qquad (3)$$

This includes some intermolecular interactions, i.e. those not included in the previous potentials.

The values for the Lennard–Jones parameter ε_{ij} for each cut-off distance are given in Table I, σ_{ij} had a value of 3.93 Å regardless of cut off distance.

Simulation Details

Simulations were carried out using a molecular dynamics code, DL Poly[‡] with a time step of 0.005 ps. The simulation cell had dimensions of 56.87 × 56.87 × 180.00 Å^3 with periodic boundary conditions in all directions, and consisted of 507 of either 10

carbon (decane) or 9 carbon (nonane) chains. The lattice chains were arranged in a slab geometry with vacuum on either side.

The lattice was melted and heated to 500 K to provide the starting configuration for the simulation at each temperature which consisted of a 100,000 step equilibration period (for the temperatures 298 and 350 K this was increased to 200,000 steps) followed by a 100,000 step production phase.

In order to determine the density of the liquid and vapour phases the density across the cell was calculated after each step and averaged over the production phase.

$$\rho_{(z)} = 1/2(\rho_L + \rho_V) - 1/2(\rho_L - \rho_V)$$

$$\times \tanh[(z - z_0)/d] \qquad (4)$$

The resulting density profile was then fitted to Eq. (4) to give ρ_L and ρ_V, the liquid and vapour densities respectively, z_0 the position of the interface and d the width of the interface.

The surface tension was calculated at each time step from the average normal and tangential pressure tensors using Eq. (5), where P_{xx}, P_{yy} and P_{zz} are the average pressure tensors in the various directions and l is the length of the simulation cell.

$$\gamma_{lv} = 1/2[P_{zz} - 1/2(P_{xx} + P_{yy})]l \qquad (5)$$

This was then averaged over the production phase. The error in the surface tension was calculated from the instantaneous values of γ_{lv} by taking subaverages $\langle\gamma\rangle$ of length τ_b and number n_b so that $\tau_{\text{run}} = \tau_b n_b$ with variance,

$$\sigma^2(\langle\gamma_{lv}\rangle_b) = \frac{1}{n_b}\sum_{b=1}^{n_b}(\langle\gamma_{lv}\rangle_b - \langle\gamma_{lv}\rangle_{\text{run}})^2 \qquad (6)$$

By plotting $\tau_b^{1/2}$ against s where

$$s = \lim_{\tau_b \to \infty}\frac{\tau_b\sigma^2(\langle\gamma_{lv}\rangle_b)}{\sigma^2(\gamma_{lv})} \qquad (7)$$

the value of the statistical inefficiency can be estimated as the limiting value of s (s_{lim}) as τ_b goes to infinity. Hence the error in the whole run becomes

$$\sigma(\langle\gamma_{lv}\rangle_{\text{run}}) = (s_{\text{lim}}/\tau_{\text{run}})^{1/2}\sigma(\gamma_{lv}) \qquad (8)$$

where $\sigma(\gamma_{lv})$ is the RMS fluctuation in the entire run [31].

[†]Most of the simulations were performed without the long range correction. This has no effect on the reported properties which are related to derivatives of the potential. The use of switching functions to take the potential smoothly to zero at r_{cut} would change the parameters derived here for short range potentials and does not appear to be necessary for our purposes.

[‡]DL_POLY is a package of molecular simulation routines written by W. Smith and T.R. Forester, copyright The Council for the Central Laboratory of the Research Councils, Daresbury Laboratory at Daresbury, UK (1996).
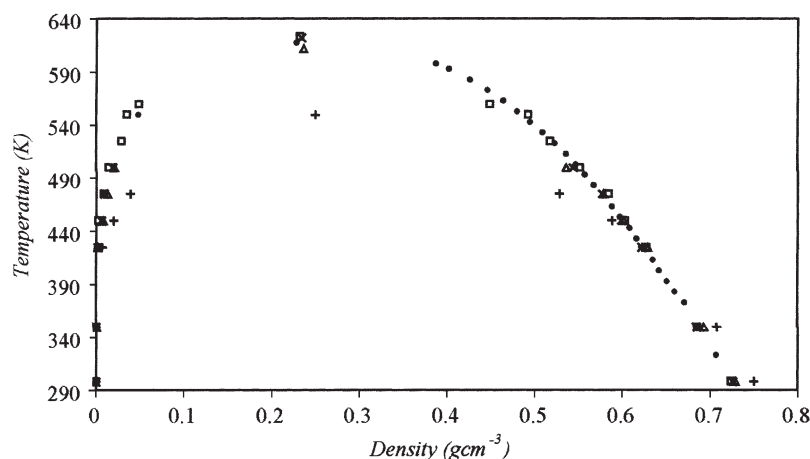
FIGURE 1 Liquid–vapour phase diagram for decane comparing results for different cut offs with experimental values. The filled circles (•) correspond to the experimental values [34,35,37] and the other symbols represent the various values of the cut-off, R_c. 13.8 Å (□), 11.0 Å (×), 8.0 Å (Δ), 6.0 Å (+).

RESULTS

Phase diagrams for decane using a range of cut-offs less than or equal to 13.8 Å were produced (see Fig. 1). At each value of the cut-off, the experimental and simulated phase diagrams were compared and new values of the LJ's parameters ε_{ij} were calculated by scaling to force agreement at a given density using Eq. (9) applied at constant liquid density.

$$\varepsilon_{\text{new}} = \frac{T_{\text{Exp}}}{T_{\text{Sim}}} \varepsilon_{\text{old}} \qquad (9)$$

This was done for a range of temperatures and the new values of the ε_{ij} parameters averaged. These values were then used to produce another liquid–vapour curve, the process being repeated until the results reproduced the experimental data within acceptable errors.

It can be seen from Fig. 1 that reducing the cut off and then rescaling epsilon has little effect on the

shape of the curve down to and including $R_c = 8.0$ Å. Once the cut off was reduced to 6.0 Å the liquid–vapour co-existence curve changed shape and became flattened causing an over estimation of the liquid density at low temperatures and an under-estimation at high temperatures. A plot of the difference between the simulated and experimental densities is given in Fig. 2.

The difference in the values for the three longest cut-offs is around zero, the 6.0 Å cut-off moves from a large positive value at the lowest temperature to a large negative one at the highest. The lowest value of the cut-off, which still gives reasonable phase co-existence data, is 8.0 Å. The LJ parameters giving the best correlation with experimental data for the 8 Å cut-off were then run with nonane. The results can be seen in Fig. 3, the model at the 8.0 Å cut off is also applicable to nonane particularly away from the critical point.

Figure 4 shows the interfacial surface tension (γ_{lv}) plotted against temperature for each cut off distance.
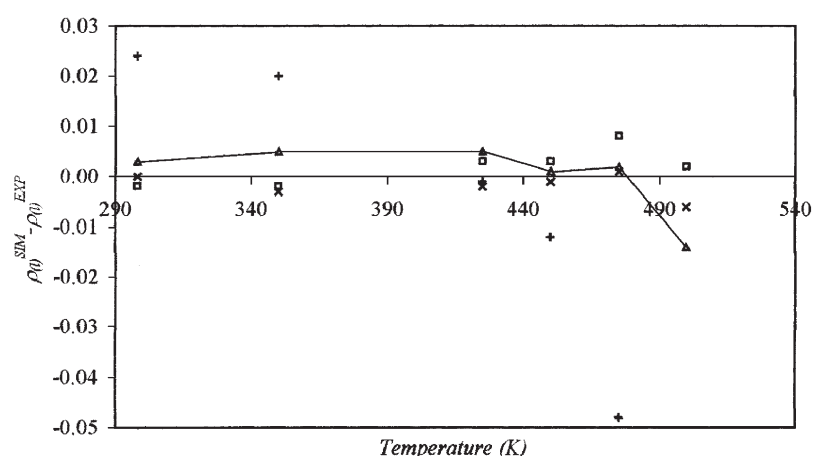

FIGURE 2 The difference between the simulated and experimental liquid densities plotted against temperature. The symbols correspond to the various values of the cut-off, R_c. 13.8 Å (□), 11.0 Å (×) 8.0 Å (Δ), 6.0 Å (+).
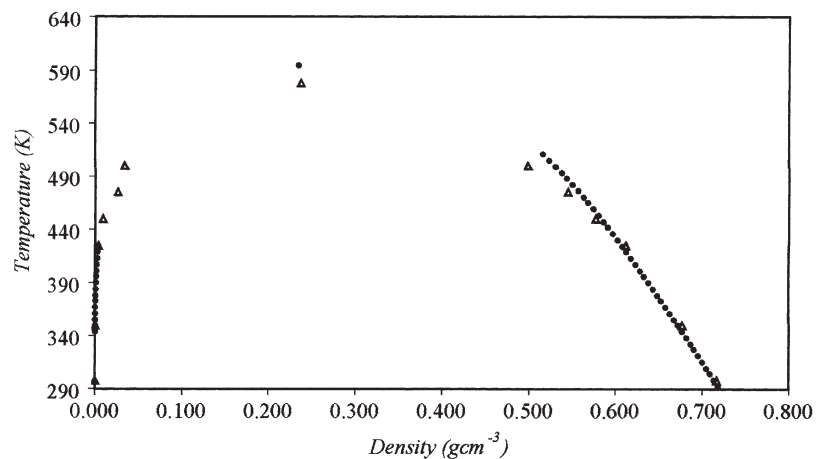
FIGURE 3   Liquid–vapour diagram for nonane. The filled circles (•) correspond to the experimental values [36,37] and the open triangles (Δ) represent the 8.0 Å cut-off.
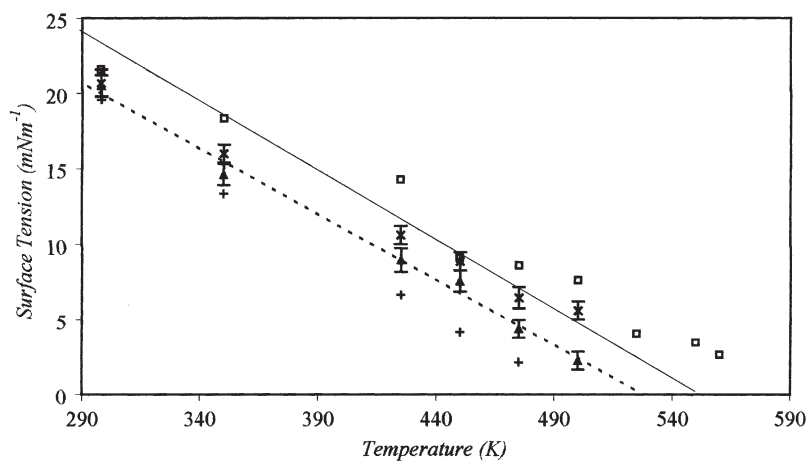

FIGURE 4   Surface tension (γ) against temperature for decane at each cut off value. The unbroken line corresponds to the experimental values [37] and the symbols represent the various values of the cut-off, R_c. 13.8 Å (□), 11.0 Å (Δ), 8.0 Å (Δ), 6.0 Å (+).The broken line is a straight line fit to the 8.0 Å data. Error bars are shown for the 8.0 and 11.0 Å data.
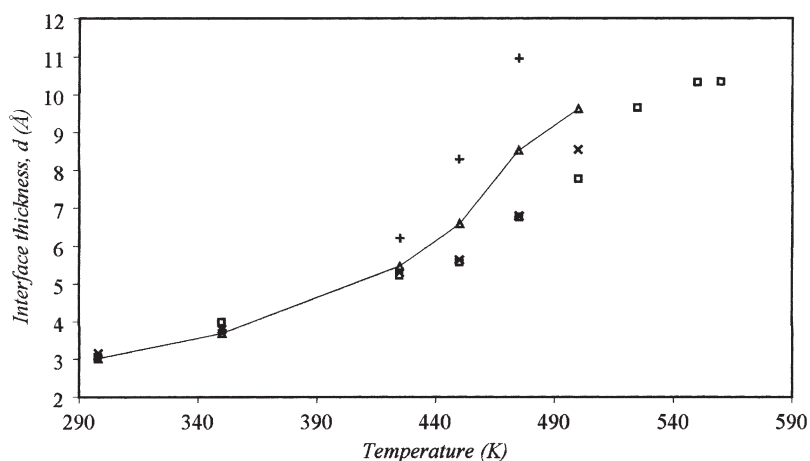

FIGURE 5   Interface thickness plotted against temperature. The symbols correspond to the various values of the cut-off, R_c. 13.8 Å (□). 11.0 Å (×), 8.0 Å (Δ), 6.0 Å (+).
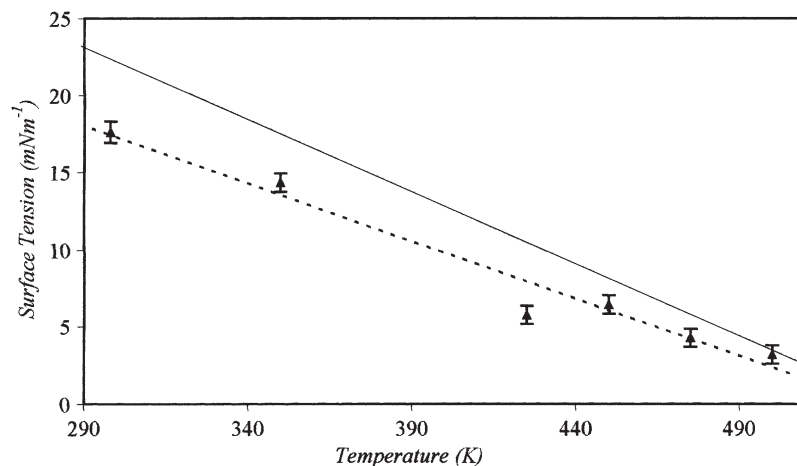
FIGURE 6 Surface tension (γ) against temperature for nonane. The unbroken line corresponds to the experimental values [37] and the open triangles (Δ) represent the 8.0 Å cut-off with error bars. The broken line is a straight line fit to the 8.0 Å data.

The longest ($R_c = 13.8$ Å) tends to over estimate the surface tension. As the cut off distance is reduced and ε is scaled accordingly there is a tendency towards lower values for the surface tension. The shortest cut off (6.0 Å) gives values significantly lower than those seen experimentally. Of the two intermediate cut-off distances the 11.0 Å values gives the best correlation with experiment. The 8.0 Å cut-off performs adequately giving reasonable values and a fit to a slope whose gradient is very close to that of the experimental curve. The interfacial thickness is plotted in Fig. 5. The simulations are in good agreement with each other until $T \sim 425$ K. The surface tension plot for nonane (see Fig. 6) is similar to that for decane, although there is a slight deviation in the slope of the simulation curve.

The model along with the 8.0 Å cut off was further tested by calculating the vapour pressure as a function of temperature. The normal vapour pressure (P_N) across the cell is given by [32].

$$P_N(z) = \langle \rho(z) \rangle kT$$

$$-\frac{1}{A} \left\langle \sum_{i<j}^{N} \sum_{a}^{n} \sum_{b}^{n} \frac{z_{ij}z_{iajb}}{r_{iajb}} \frac{dU(r_{iajb})}{dr_{iajb}} \frac{1}{|z_{ij}|} \right.$$

$$\left. \times \theta\left(\frac{z-z_i}{z_{ij}}\right) \theta\left(\frac{z_j-z}{z_{ij}}\right) \right\rangle \qquad (10)$$

where Z_i is the z coordinate of the centre of mass of molecule i and θ is a unit step function.

To calculate the vapour pressure runs of 200,000 steps were started from pre-equilibrated states. Every 50 steps the normal pressure profiles were calculated using Eq. (10) and these averaged over blocks of 10,000 steps. The value of the vapour pressure was taken as the average value of the normal pressure in the vapour phase throughout the entire run. The results in Fig. 7 show good agreement with the experimental data although there is some deviation at lower temperatures.

Table II contains a comparison between the data of Smit *et al.* [12], using the model on which this study is based, and our short range (8 Å) potential. The new potential is slightly more accurate than the longer ranged version and is applicable in a wider temperature range $298 < T < 500$ K.

CONCLUSIONS

Our united atom model with an 8.0 Å cut-off gives an acceptable description of the liquid–vapour phase diagram and interfacial properties of the alkanes, decane and nonane. It is comparable in accuracy to other "longer range" models (See Table II). Further
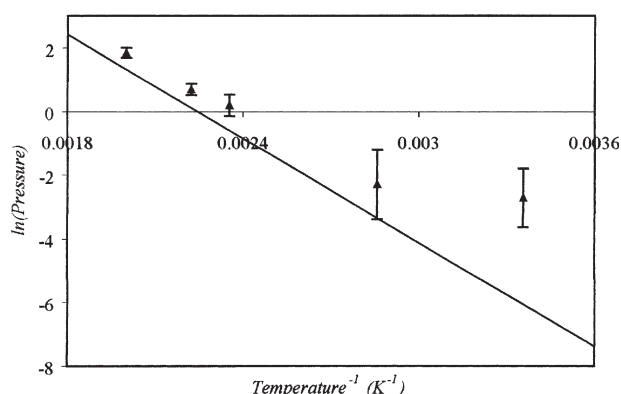

FIGURE 7 The normal pressure tensor averaged throughout the vapour phase for decane and presented as a Clapeyron plot. The line corresponds to the experimental values [37] and the open triangles (Δ) represent the 8.0 Å cut-off with error bars.

TABLE II   Comparison of the liquid density data for decane between the results of Smit *et al.* [12] and those of the short range potential reported here

	Temperature (K)	298	350	425	450	475	500
Smit *et al.* [12]	% Dev. from exp.			0.64	0.83	0.35	3.45
	Avg. % Dev. from exp.					1.28	
Short range potential	% Dev. from exp.	0.41	0.73	0.80	0.17	0.35	2.55
	Avg. % Dev. from exp.*					0.97	
	Avg. % Dev. From exp.			0.84			

*Using the densities where $T > 350\,K$, for direct comparison.

reduction of the cut-off distance results in strong deviations from the liquid–vapour coexistence curve. These potentials will enable efficient simulations of fluid phase behaviour such as wetting by alkanes [33] where there is a need to minimise time spent computing fluid–fluid interactions.

Acknowledgements

References

[1] Goodman, J.M. (1997) "What is the longest unbranched alkane with a linear global minimum conformation?", *J. Chem. Inf. Comput. Sci.* **17**, 876.
[2] Van der Ploeg, P. and Berendsen, H.J.C. (1982) "Molecular-dynamics simulation of a bilayer-membrane", *J. Chem. Phys.* **76**, 3271.
[3] Chiu, S.W., Clark, M.M., Jokobsson, E., Subramaniam, S. and Scott, H.L. (1999) "Optimization of hydrocarbon chain interaction parameters: Application to the simulation of fluid phase lipid bilayers", *J. Phys. Chem. B* **103**, 6323.
[4] Jin, B.Q. and Hopfinger, A.J. (1997) "Characterization of lipid membrane dynamics by simulation. 1. Torsion angle motions of the linear chains", *Biopolymers* **41**, 37.
[5] Zhang, Xiu-bin, Li, Ze-sheng, Lu, Zhong-yuan and Sun, Chia-chung (2001) "Molecular dynamics simulation of the linear low density polyethylene crystallization", *J. Chem. Phys.* **115**, 3916.
[6] Taylor, D.J.R., Stepto, R.F.T., Jones, R.A. and Ward, I.M. (1999) "Computer simulation studies of molecular orientation and the stress-optical properties of polyethylene networks", *Macromolecules* **32**, 1978.
[7] McGann, M.R. and Lacks, D.J. (1999) "Entropically induced Euler buckling instabilities in polymer crystals", *Phys. Rev. Lett.* **82**, 952.
[8] Lacks, D.J. and Rutledge, G.C. (1994) "Simulation of the temperature-dependence of mechanical-properties of poly-ethylene", *J. Phys. Chem.* **98**, 1222.
[9] Meunier, M. and Quirke, N. (2000) "Molecular modelling of electron trapping in polymer insulators", *J. Chem. Phys.* **113**, 369.
[10] Anta, J.A., Marcelli, G., Meunier, M. and Quirke, N. (2002) "Models of electron trapping and transport in polyethylene: Current–voltage characteristics", *J. Appl. Phys. D* **92**, 1002.
[11] Goujon, F., Malfreyt, P., Boutin, A. and Fuchs, A.H. (2001) "Vapour–liquid phase equilibria of n-alkanes by direct Monte Carlo simulations", *Mol. Sim.* **27**, 99.
[12] Smit, B., Karaborni, S. and Siepmann, J.I. (1995) "Computer simulations of vapor–liquid phase equilibria of n-alkanes", *J. Chem. Phys.* **102**, 2126.
[13] Nath, S.K., Escobedo, F.A. and de Pablo, J.J. (1998) "On the simulation of vapour–liquid equilibria for alkanes", *J. Chem. Phys.* **108**, 9905.
[14] Martin, M.G. and Siepmann, J.I. (1998) "Transferable potentials for Phase Equilibria. 1. United-Atom Description of n-alkanes", *J. Phys. Chem. B* **102**, 2569.
[15] Quirke, N. (1996) "Predict fluid phase equilibria using molecular simulation", *Chem. Eng. Prog.* **92**, 65.
[16] Ungerer, P., Boutin, A. and Fuchs, A.H. (2001) "Direct calculation of bubble points for alkane mixtures by molecular simulation", *Mol. Phys.* **99**, 1423.
[17] Neubauer, B., Delhommelle, J., Boutin, A., Tavitian, B. and Fuchs, A.H. (1999) "Monte Carlo simulations of squalane in the Gibbs ensemble", *Fluid Phase Equilib.* **155**, 167.
[18] Schuler, L.D. and van Gunsteren, W.F. (2000) "On the choice of dihedral angle potential energy functions for n-alkanes", *Mol. Sim.* **25**, 301.
[19] Delhommelle, J., Millie, P. and Fuchs, A.H. (2000) "On the role of the definition of potential models in Gibbs ensemble phase equilibria simulations of the H2S-pentane mixture", *Mol. Phys.* **98**, 1895.
[20] Mackie, A.D., Tavitian, B., Boutin, A. and Fuchs, A.H. (1997) "Vapour–liquid phase equilibria predictions of methane–alkane mixtures by Monte Carlo simulation", *Mol. Sim.* **19**, 1.
[21] Hansen, F.Y., Newton, J.C. and Taub, H. (1993) "Molecular dynamics studies of the melting of butane and hexane monolayers adsorbed on the basal-plane surface of graphite", *J. Chem. Phys.* **98**, 4128.
[22] de Gennes, P.G. (1985) "Wetting: statics and dynamics", *Rev. Mod. Phys.* **57**, 827.
[23] Grunze, M. (1999) "Surface science-driven liquids", *Science* **283**, 5398.
[24] Ryckaert, A. (1975) "Molecular dynamics of liquid n-butane near its boiling point", *Chem. Phys. Lett.* **30**, 123.
[25] Paul, W., Yoon, D.Y. and Smith, G.D. (1995) "An optimized united atom model for simulations of polymethylene melts", *J. Chem. Phys.* **103**, 1702.
[26] Neubauer, B., Boutin, A., Tavitian, B. and Fuchs, A.H. (1999) "Gibbs ensemble simulations of vapour–liquid phase equilibria of cyclic alkanes", *Mol. Phys.* **97**, 769.
[27] Toxvaerd, S. (1990) "Molecular dynamics calculation of the equation of state of alkanes", *J. Chem. Phys.* **93**, 4290.
[28] Toxvaerd, S. (1997) "Equation of state of alkanes. 2", *J. Chem. Phys.* **107**, 5197.
[29] Ungerer, P., Beauvais, C., Delhommelle, J., Boutin, A., Rousseau, B. and Fuchs, A.H. (2000) "Optimization of the anisotropic united atoms intermolecular potential for n-alkanes", *J. Chem. Phys.* **112**, 5499.
[30] Van der Ploeg, P. and Berendsen, H.J.C. (1982) "Molecular-dynamics simulation of a bilayer-membrane", *J. Chem. Phys.* **76**, 3271.
[31] Allen, M.P. and Tildesley, D.J. (1987) *Computer Simulation of Liquids* (Oxford University Press, Oxford).
[32] Alejandre, J., Tildesley, D.J. and Chapela, G.A. (1995) "Fluid phase equilibria using molecular dynamics: the surface tension of chlorine and hexane", *Mol. Phys.* **85**, 651.
[33] Supple, S., Quirke, N. (Work in progress).
[34] Francis, A.W. (1957) "Pressure–Temperature–Liquid Density Relations of Pure Hydrocarbons", *Ind. Eng. Chem.* **49**, 1779.
[35] Gehrig, M. and Lentz, H. (1983) "Values of $p(V_m,T)$ for n-decane up to 300 MPa and 673 K", *J. Chem. Thermodyn.* **15**, 1159.
[36] Smith, B.D. and Srivastava, R. (1986) *Thermodynamics of Pure Compounds: Hydrocarbons and Ketones* (Elsevier, New York).
[37] Lide, D.R., ed, (1993) *Handbook of Chemistry and Physics*, 74th Ed. (CRC Press, Florida).